STUDY OF A TRIPLE-LAYER PHOSWICH DETECTOR FOR BETA AND GAMMA SPECTROSCOPY WITH MINIMAL CROSSTALK

A. T. Farsoni and D. M. Hamby

Oregon State University

Sponsored by National Nuclear Security Administration
Office of Nonproliferation Research and Development
Office of Defense Nuclear Nonproliferation
and
Department of Energy

Contract Nos. DE-FC52-06NA27322 and DE-FG07-02ID14331

ABSTRACT

The Automated Radioxenon Sampler/Analyzer (ARSA) has been developed at Pacific Northwest National Laboratory for the Comprehensive Nuclear-Test-Ban Treaty (CTBT) to monitor radioactive xenon. Employing 12 photomultiplier tubes in the present ARSA technology makes it calibration intensive and power hungry. Therefore, to be used at remote distances and as an unattended system, simplification of the current ARSA is essential.

A triple-layer phoswich detector has been developed at Oregon State University to collect separate beta and gamma energy spectra with minimal crosstalk. By utilizing a digital pulse processing scheme, the detector is also capable of recording coincidence events and therefore can be used to simplify the ARSA technology. The first two layers, CaF_2 and BC400, are chosen specifically for beta spectroscopy and the third layer, NaI, is intended for gamma-ray spectroscopy. The Monte Carlo n-particle (MCNP) code was used to simulate energy deposition in each layer from gamma-rays and monoenergetic electrons. In this paper, we discuss the MCNP analysis and preliminary experimental results, in which digital signal processing techniques are employed.

OBJECTIVE

The ARSA has been developed at the Pacific Northwest National Laboratory to measure the four radioxenons ^{131m}Xe, ^{133m}Xe, ^{133}Xe and ^{135}Xe released after a nuclear weapons test (Reeder and Bowyer, 1998). The ARSA system is intended to be employed in the International Monitoring System (IMS) as part of the Comprehensive Nuclear-Test-Ban Treaty. The ARSA system uses two separate channels for beta and gamma detection in a coincidence scheme to significantly reduce the natural background. The beta channel includes two photomultiplier tubes (PMTs) per gas cell, a total of 8 PMTs, for detecting beta absorption in cylindrical plastic scintillators. The gamma channel has four photomultiplier tubes for detecting any gamma deposition in two NaI(Tl) crystals. Although very sensitive, employing 12 photomultiplier tubes in one compact system requires a continuous and precise calibration. In addition to the calibration difficulties, the ARSA system needs a substantial source of power. To overcome these limitations, several efforts were initiated to investigate employing one single channel for both beta and gamma detection using phoswich detectors.

A phoswich detector developed by Ely et al., (2003) consisted of two scintillation layers, a CaF_2(Eu) layer (decay constant 940 ns) and a NaI(Tl) layer (decay constant 230 ns) intended for beta and gamma detection, respectively. The scintillation layers were optically coupled to a single PMT with an integrating preamplifier. Then rising pulses from the preamplifier were digitally captured and analyzed. Another phoswich detector design was introduced by Hennig et al., (2005). This phoswich design also had two layers, plastic scintillator BC-404 (decay constant 1.8 ns) and CsI(Tl) crystal (with two decay constants of 0.68 and 3.34 μs) optically coupled to a single PMT. The signal output from the PMT was directly connected to a digital pulse processor. Because radiation pulses are not integrated but are directly captured, the timing profile of pulses represents the timing profile of light produced in each scintillation layer.

By choosing a sufficient density thickness of CaF_2(Eu), 324 mg/cm^2, Ely's phoswich is designed to stop nearly the highest beta particle energies from radioxenon decay (905 keV from ^{135}Xe). This enhances the beta spectroscopy capability, but increases the Compton scattering probability and introduces some degree of crosstalk from the incident gamma rays in that layer. On the other hand, to reduce the probability of interaction of the incident gamma rays with the plastic scintillator in the design of Hennig et al., (2005) the density thickness is reduced to 103 mg/cm^2, stopping 362 keV electrons.

In this paper, we introduce a triple-layer phoswich detector which is able to collect separate gamma and beta energy spectra simultaneously with minimal crosstalk. The MCNP code was used to predict the probability of possible pulse shapes from gamma and beta interactions with the detector layers. We also discuss the preliminary results in which the detector was exposed to pure beta (^{90}Sr/^{90}Y) and gamma (^{137}Cs) sources to examine the ability of the detector to separate beta-only and gamma-only pulses.

RESEARCH ACCOMPLISHED

Phoswich Detector Design

A triple-layer phoswich detector is designed for simultaneous gamma and beta spectroscopy. Having sufficient timing contrast and low Z elements, the first two layers, BC-400 and CaF_2(Eu), are chosen specifically for beta particle spectroscopy. The third layer, NaI(Tl), is intended for gamma-ray spectroscopy. The schematic arrangement of the detector and the physical properties of the scintillation materials are shown in Figure 1 and Table 1, respectively.

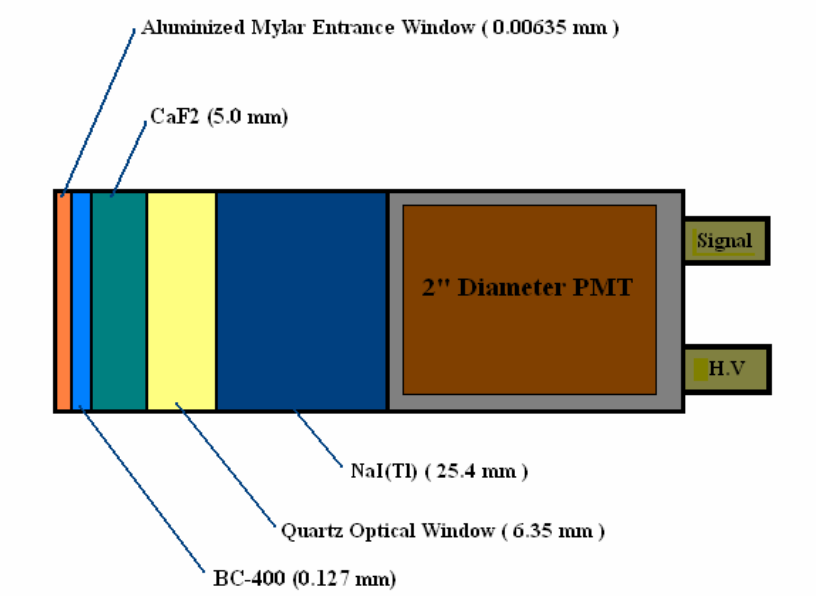

Figure 1. Schematic arrangement of the phoswich detector.

Table 1. Physical properties for scintillation materials used in the phoswich detector.

Scintillator	Density (g/cm^3)	Max. Emission Wavelength (nm)	Light Output (% of NaI)	Index of Refraction	Principle Decay Constant (ns)
BC-400	**1.032**	**423**	**26**	**1.58**	**2.4**
CaF_2:Eu	**3.19**	**435**	**50**	**1.47**	**900**
NaI:Tl	**3.67**	**415**	**100**	**1.85**	**230**

Since NaI(Tl) is a hygroscopic crystal, it is isolated from the other two components by a quartz optical layer. The density thickness of BC-400 and CaF_2(Eu) together are such that electrons with energies up to 3.2 MeV are stopped in these layers. As it will be shown in MCNP simulation of the detector, the light component from the fast scintillator, BC400, acts as a passive signature of the beta-induced pulses. If the incident electron has enough energy to penetrate into the slow scintillator, CaF_2(Eu), the two simultaneous light pulses form a double-component pulse at the photomultiplier output. Employing an appropriate digital pulse processing algorithm, this type of pulse can be separated from gamma-induced-pulses which are generated from interaction of gamma rays either in CaF_2(Eu) (mostly from Compton scattering) or in NaI(Tl). Since only very high energy electrons (6.7 MeV) can penetrate into the NaI(Tl) crystal, the light pulses (decay time 230 ns) generated in this layer represent only gamma ray interactions with no crosstalk from beta particle energy absorption.

MCNP Simulation

The MCNP code was used to simulate energy deposition from gamma-rays and monoenergetic electrons in each layer of the detector. It should be noted that, for all probability calculations using MCNP, the energy threshold was assumed to be 10 keV so that events with energies less than this amount were excluded.

Figures 2(a) and 2(b) show two simulated energy deposition spectra from 1 MeV gamma rays in the three scintillation layers and from different monoenergetic electrons in BC-400, respectively. From Figure 2(a) as expected, Compton scatter is the prominent interaction from incident gamma rays in BC400 and CaF_2(Eu). The legend in Figure 2(a) also shows the total interaction probabilities (TP) from 1 MeV gamma rays in each layer.

Since the CaF_2(Eu) layer is thick enough to accommodate electrons up to 3.2 MeV, the unwanted events (mostly Compton scattering) in the beta-side of the detector (CaF_2 (Eu)) are comparable to that of the gamma-side, the NaI(Tl) layer. However, since common beta particles have much shorter mean free paths than gamma rays in scintillation materials, events in the first layer can be used to identify the beta-induced pulses from beta interactions with CaF_2 (Eu), and so the Compton events can be distinguished quite easily. Figure 2(b) shows how the fast light component (2.4 nsec) from the first layer behaves when the layer is exposed to different monoenergetic electrons. With increasing energy of electrons above 100 keV, the most significant component of the spectra shifts towards lower energies. In terms of anode pulse shape, this means that electrons with energies higher than a threshold most likely add a small amount of fast decay component to the generated signal pulse.

By combining three timing components corresponding to the decay constants of three scintillation layers and depending on how a given incident beta or gamma ray releases its energy within each layer, seven possible interaction scenarios for either beta or gamma interactions could occur (Farsoni and Hamby, 2005). Corresponding to these scenarios, seven possible pulse shapes can be generated. The occurrence probabilities for seven possible gamma- and beta-induced pulse types, calculated using the MCNP code, are given in Table 2. These results provide the criteria for acceptance of a pulse as a beta only, gamma only or beta/gamma coincidence pulse.

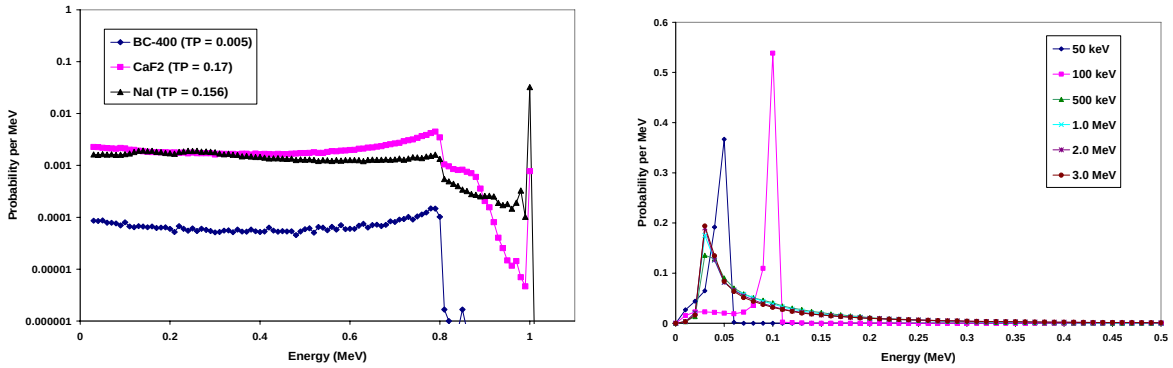

(a) (b)

Figure 2. Simulated energy spectra from (a) 1.0 MeV gamma rays in three layers and (b) different monoenergic electrons in BC-400.

Table 2. Pulse acceptance/rejection criteria calculated using MCNP simulation. *Total probabilities are calculated for 1.0 MeV photon/electron events. Events with energies less than 10 keV were excluded as electronic noise.

Scenario	Scintillation Layers			Total Probability (%)*		Pulse Recorded as:
	BC-400	CaF2	NaI:Tl	Gamma	Beta	
1	×			0.35	**12.30**	**Beta Only**
2	×	×		0.07	**81.70**	
3		×		14.40	4.60	Rejected
4	×		×	0.06	0.08	**B/G Coincidence**
5		×	×	2.65	0.03	Rejected
6	×	×	×	0.01	0.57	**B/G Coincidence**
7			×	**12.87**	0.00	**Gamma Only**

For example, if a pulse is observed with only the fast component (pulse type 1) or both fast and slow components (pulse type 2, Figure 3(a)), the probability that the pulse is gamma-induced is 0.35% or 0.07%, respectively, whereas the probability for a beta particle with the same energy producing the same pulse type is 12.30% or 81.70%, respectively. Therefore, these types of pulses update the corresponding beta particle energy histogram. However, if a pulse is observed as having only a decaying component corresponding to the energy deposition in the NaI(Tl) (pulse type 7, Figure 3(b)), the probability that the pulse is from a 1 MeV gamma ray or beta particle is 12.87% or 0.00%, respectively. This type of pulse, therefore updates the corresponding gamma-ray energy histogram. When the radionuclide emits both beta and gamma rays, gamma/beta coincident pulses can be detected from pulse types 4 and 6. Since there is no useful information in pulse types 3 and 5, these pulses are not recorded.

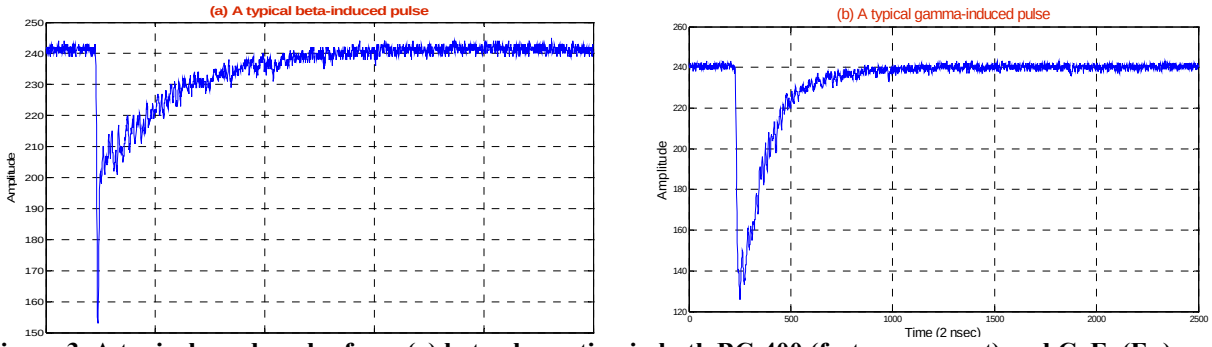

Figure 3. A typical anode pulse from (a) beta absorption in both BC-400 (fast component) and CaF_2 (Eu) (slow component), and (b) gamma absorption in NaI(Tl).

Development of an Algorithm for Gamma/Beta Separation

Based on the MCNP simulation results, an off-line algorithm is developed to digitally process the anode pulses and collect separate beta and gamma energy spectra. To develop the algorithm at this phase of our study, pulse types 1, 2 and 7 (beta- and gamma-only events) are detected but pulse types 4 and 6 (beta/gamma coincidence events) are not considered.

For each pulse, four sums, Base, A, B and C, are calculated (Figure 4). For the baseline determination, the average of Base is used. A simplified flowchart of the algorithm is shown in Figure 6. After loading the waveform and the baseline correction, using the peak of waveform and the average of sum B, the fast ratio (FR) of the pulse is measured. The FR quantity indicates the presence of a fast component in the pulse. Then FR is compared with a threshold value, FR_th. If the pulse passes the inspection, the pulse is considered to be a beta-induced candidate pulse, otherwise it is processed as a gamma-induced pulse candidate. Figure 5 shows the measured FR distribution from two pure beta emitters, $^{90}Sr/^{90}Y$ and ^{36}Cl, and two gamma sources, ^{137}Cs and ^{60}Co. For the preliminary experiments, FR_th was chosen to be around 0.35.

To be accepted as a beta- or gamma-induced pulse, the pulse should pass another inspection, the fall time measurement. In the beta case, the fall time measurement is done only on the slow part of the pulse and then the result is compared with a fall time threshold. If the result is positive, using sums A and C, the corresponding beta energy deposition in BC-400 and CaF_2(Eu) is calculated and the beta energy histogram is updated. In the gamma case, if the fall time is within a fall time window, using sum C, the corresponding gamma energy deposition in NaI(Tl) is calculated and the gamma energy histogram is updated.

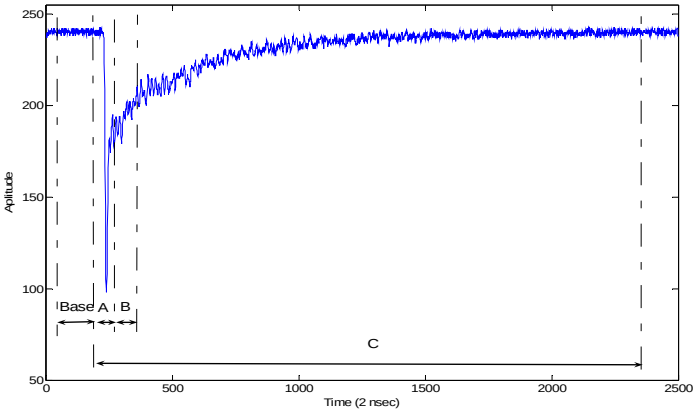

Figure 4. Four sum regions—Base, A, B and C—used to analyze the anode pulses.

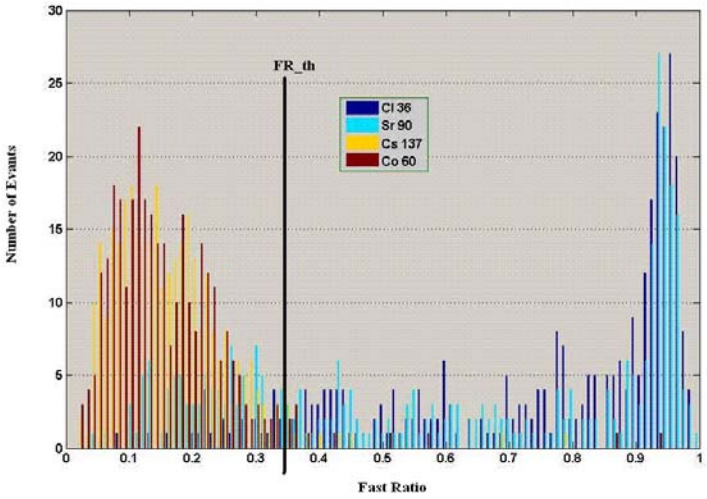

Figure 5. FR distribution from four beta and gamma sources. Detector was shielded against beta/conversion electrons when exposed to gamma sources.

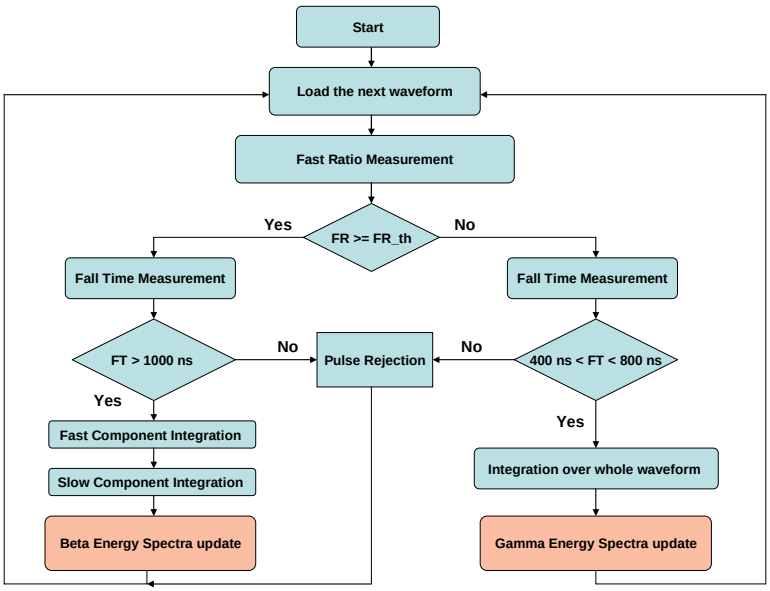

Figure 6. The algorithm developed to collect separate gamma and beta energy spectra.

Simultaneous Beta/Gamma Spectroscopy

Using a digital oscilloscope with 500 MSPS sampling rate and 8-bit resolution, anode pulses were captured directly and then transferred to the PC through the serial (RS-232) port. To evaluate how the algorithm separates gamma and beta events, the phoswich detector was exposed on separate occasions to $^{90}Sr/^{90}Y$, ^{14}C and ^{137}Cs sources. Beta particles and conversion electrons from ^{137}Cs were blocked using an appropriate shield during counting. Results are shown in Figure 7.

Three scintillation layers with relatively high light output differences (in Table 1, max light output ratio is 100/26) in a single light channel expands the dynamic range of the anode output. Therefore, for a higher degree of precise digital measurements, employing an analog-to-digital converter (ADC) with lower quantization errors is necessary. We believe that the relatively high fraction of accepted gamma and beta events, respectively from pure beta and gamma sources, results from over-or-under estimation of either the FR or fall time measurements.

The high difference in the percentage of rejected gamma events in Figures 7(a) and 7(b) can be explained using the MCNP analysis presented in Figure 2(b). On average, beta particles from $^{90}Sr/^{90}Y$ deposit less energy than that of ^{14}C in the BC-400 layer. This produces relatively smaller fast components in the induced pulses from $^{90}Sr/^{90}Y$ and subsequently causes the Fast Ratio algorithm to misclassify some of them as a gamma candidate pulse. Eventually, the misclassified pulses are rejected in the fall time inspection. These fractions, however, can be significantly modified using a digital data acquisition system with higher resolution, i.e., 12 bits. The rejected gamma events from the gamma source, 10.7%, are believed to be mostly from Compton scatter in $CaF_2(Eu)$.

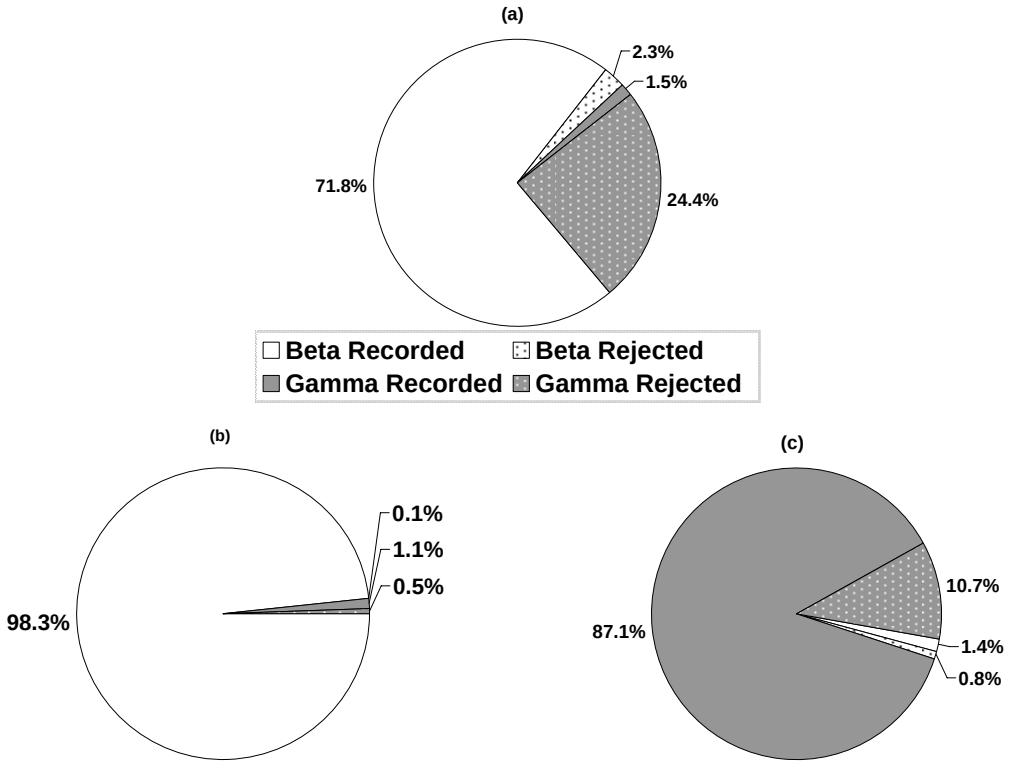

Figure 7. Percentage of events when the detector was exposed separately to (a) pure beta $^{90}Sr/^{90}Y$, (b) ^{14}C, and (c) shielded gamma (^{137}Cs) sources.

Figure 8 shows the separated beta and gamma spectra when the phoswich detector is exposed to both $^{90}Sr/^{90}Y$ and ^{137}Cs sources simultaneously. Again beta particles and conversion electrons from ^{137}Cs were blocked during spectroscopy.

The beta and gamma energy absorption spectra in Figure 8 possess details as expected. For example, in the gamma spectrum, the photopeak has a nearly symmetric shape (FWHM ~ 8%) and the Compton continuum and Compton edge are prominent. The shape of the beta spectrum is similar to that expected from $^{90}Sr/^{90}Y$ in that two components can be seen. Some energy degradation is apparent and could result from energy absorption in air and the Mylar layer, energy absorption in the gap between the BC-400 and $CaF_2(Eu)$ scintillators, and incomplete beta particle absorption and backscattering in the material interfaces.

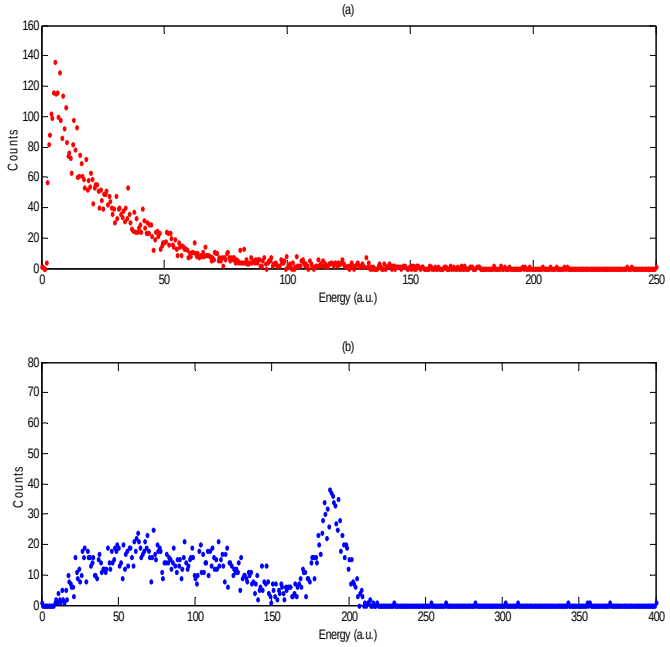

Figure 8. Simultaneous beta (a) and gamma (b) energy spectra digitally collected and processed from 15,000 anode pulses when the detector was exposed to both $^{90}Sr/^{90}Y$ and ^{137}Cs sources.

CONCLUSION

A triple-layer phoswich detector for simultaneous beta and gamma ray spectroscopy was simulated and built. Based on the criteria extracted from the MCNP analysis, an algorithm was developed to separate beta- and gamma-induced pulses in the BC-400/CaF_2(Eu) and NaI(Tl), respectively. A fast digital oscilloscope was used to capture and transfer anode pulses to the PC. The preliminary experimental results proved the overall concept of the detector design as a general purpose beta/gamma detector. The second phase of this research includes optimizing the phoswich detector for radioxenon detection and employing a customized digital pulse processor with 100 MSPS and 12-bit resolution to apply the detector capabilities for radioxenon beta/gamma coincidence.

ACKNOWLEDGEMENTS

We would like to thank the United States Department of Energy, Nuclear Engineering Education Research and the National Nuclear Security Administration, for sponsorship of portions of this work.

REFERENCES

Reeder, P. L., T. W. Bowyer, and R. W. Perkins (1998). Applications of nuclear techniques to non-proliferation treaties and weapons detection—Beta-gamma counting system for Xe fission products, *J. Radioanal. Nucl. Chem.* 235: 89–94.

Ely, J. H., C. E. Aalseth, J. C. Hayes, T. R. Heimbigner, J. I. McIntyre, H. S. Miley, M. E. Panisko, and M. Ripplinger, (2003). Novel beta-gamma coincidence measurements using phoswich detectors, in *Proceedings of the 25th Seismic Research Review–Nuclear Explosion Monitoring: Building the Knowledge Base*, LA-UR-03-6029, Vol. 2, pp. 533–541.

Hennig, W., H. Tan, W. K. Warburton, and J. I. McIntyre (2005). Digital pulse shape analysis with phoswich detectors to simplify coincidence measurements of radioactive xenon, in *Proceedings of the 27th Seismic Research Review–Nuclear Explosion Monitoring Technologies,* LA-UR-05-6407, Vol. 2, pp. 787–794.

Farsoni, A. T. and D. M. Hamby (2005). MCNP analysis of a multilayer phoswich detector for beta-particle dosimetry and spectroscopy, *Nucl. Instrum. Methods Phys. Res., Sect. A*. 555: 553–559